Biophysical Chemistry 4 (1976) 113–121

SUSTAINED OSCILLATIONS AND THRESHOLD PHENOMENA IN AN OPERON CONTROL CIRCUIT

M. SANGLIER and G. NICOLIS
Faculté des Sciences de l'Université Libre de Bruxelles, Belgium

Received 11 August 1975
Revised manuscript received 27 October 1975

A genetic regulatory model involving a positive feedback (via induction) and a negative feedback (via catabolite repression) is analyzed and applied to the problem of the lac operon regulation in *E. coli*. Damped and sustained oscillations of the limit cycle type are found along with threshold phenomena corresponding to multiple limit cycles or to multiple steady states, for values of the parameters compatible with experimental data.
A comparison with the observations of Knorre and Goodwin is outlined.

1. Introduction

Open systems undergoing nonlinear kinetics and driven beyond a critical distance from thermodynamic equilibrium, may exhibit a markedly cooperative behavior beyond a transition point where the branch of solutions showing equilibrium-like behavior looses its stability [1]. The subsequently emerging *dissipative structures* may feature spatial or temporal periodicities, wave-like activity or all-or-none transitions between steady states [2].

The importance and the generality of oscillatory behavior in biochemical control processes is nowadays widely recognized [6]. Most of the dissipative structures analyzed hitherto in the context of biological regulatory processes refer to sustained oscillations of the *limit cycle* type. Systems showing this kind of behavior involve, typically, positive (like, e.g., the PFK reaction * in the glycolytic pathway [3]) or negative (like, e.g., the Yates–Pardee sequence [4]) feedback, or even a combined action of both [5].

In this paper we analyze a biochemical regulatory model which in addition to sustained oscillations and multiple steady states may present, for certain ranges of values of the parameters, *multiple limit cycles* and associated threshold phenomena. The model refers more specifically to the regulation of the lac operon in *E. coli*. Experimentally, the β-galactosidase synthesis mediated by this operon has already been shown to present oscillatory behavior under certain conditions [7].

A previous analysis of a simple model for the lac operon [8] has revealed the possibility of all-or-none transitions between multiple steady states. These transitions have been shown to correspond to the all-or-none character of the phenomenon of induction of β-galactosidase synthesis itself.

Now, in bacterial populations growing in a fixed nutrient medium with a gratuitous inducer (like IPTG) * one may reasonably expect that a *positive feedback* corresponding to the action of the permease will be the important step in the regulation of β-galactosidase activity. On the other hand if lactose (or more probably a product of the lactose catabolism) is used as inducer, the control circuit will be subject to two adverse processes. On the one side, the inducer will derepress the lac operon and exert therefore a positive feedback action. But on the other side glucose, which is a product of the lactose catabolism, can act as a catabolite repressor and be in this way a source

* PFK: phosphofrutokinase.

* IPTG: isopropylthiogalactose.

of negative feedback in the enzyme synthesis. As we shall show the combined action of these two kinds of feedback will give rise, under certain conditions on the rate constants and on the nutrient medium, to various types of oscillatory behavior, including multiple limit cycles.

The process of catabolite repression involves many steps in which c-AMP plays an important role. Here we will adopt a *global* description, wherein the (inactive) repressor binds with the catabolite repressor and gives rise to a complex whose affinity of binding with the operator is enhanced [9].

In section 2 we describe the model and develop the rate equations. Section 3 is devoted to the presentation of the results of a numerical solution of the equations supplemented with some analytical and topological considerations. Special care has been taken in the numerical simulation, to respect the experimentally known relations on the rate constants. In the final section 4 some remarks are presented on the implications of multiple limit cycle behavior in biochemical systems.

2. The model

The following control circuit (fig. 1) can reasonably be expected to describe the salient features of the regulation of the lac-operon activity

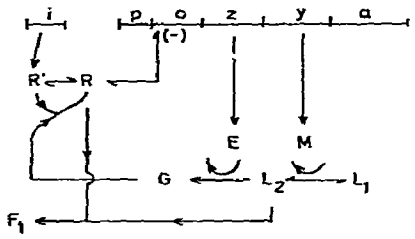

Fig. 1. Schematic representation of control circuit of the lac operon.

In terms of "chemical steps" one has

$$R' \underset{k_1'}{\overset{k_1}{\rightleftharpoons}} R \tag{1}$$

$$R' + n_G G \underset{k_2'}{\overset{k_2}{\rightleftharpoons}} R + D \tag{2}$$

$$R + n_L L_2 \underset{k_3'}{\overset{k_3}{\rightleftharpoons}} F_1 \tag{3}$$

$$R + O^+ \underset{k_4'}{\overset{k_4}{\rightleftharpoons}} O^- \tag{4}$$

$$\eta + O^+ \xrightarrow{\gamma} O^+ + E + M \tag{5}$$

$$E + L_2 \xrightarrow{k_5} E + G + F \tag{6}$$

$$M + L_1 \underset{k_6'}{\overset{k_6}{\rightleftharpoons}} M + L_2 \tag{7}$$

$$E \xrightarrow{k_7} F_2 \tag{8}$$

$$M \xrightarrow{k_8} F_3 \tag{9}$$

The first of these steps describes the equilibrium between an inactive repressor R', synthesized through the regulatory gene i, and the inactive repressor R which may block (step (4)) the operator O (form O^-). Otherwise the active operator in the form O^+ permits the synthesis, by the structural genes z and y, of the β-galactosidase, E and the permease, M (step (5)). η stands for the pool of amino-acids. Note that for simplicity, the various biosynthetic steps have been condensed into a single one. Once M is synthesized it facilitates the entry of the inducer L_1 (step (7)). This complex process is again simplified here in a single step [11]. The asymmetry of the lactose-permease binding is accounted for by taking $k_6 \gg k_6'$. Subsequently the internal inducer L_2 via a generally cooperative interaction (step (3)), inactivates the repressor (positive feedback). One the other hand, G, the product of the internal inducer's L_2 catabolism stimulates the formation of active repressor (step (2)) via another cooperative step (negative feedback). In this respect we note that it has been established [10] that the repressor is an allosteric protein formed by four monomers. The cooperative coefficient between repressor and inducer has been determined experimentally and is around two. Thus, we set in step (3) $n_L = 2$. Owing to the similarity between R and R' we also take $n_G = 2$ in step (2). Finally, steps (8) and (9) express the dilution of the two proteins in the cellular medium.

It should be pointed out that the model we have just described is a rather simplified one which only re-

tains the important aspects of the process. For instance, one knows that the repressor is an allosteric molecule which exists in two conformations, one active and one inactive. Nevertheless in writing step (1) we have merely expressed the equilibrium between the active and the inactive conformations and did not make explicit reference to the finer structure of the repressor. A detailed allosteric model has been elaborated recently [11] and shown to give rise to the same qualitative behavior as the simplified model adopted here.

We may now write the rate equations for the variables R, G, O^+, E, M, L_2. To this end we assume that R', η, L_1 are in sufficiently abundant quantities and may therefore be treated as constants. Moreover, we recall that

$$O^+ + O^- = \chi = \text{const.} \tag{10}$$

where $O^\pm$ is the *concentration* of the operator in the medium.

Assuming the system is maintained uniform in space we obtain, setting $k'_2 = \kappa'_2 D$:

$$dR/dt = k_1R' - k'_1R + k_2R'G^2 - k'_2R - k_3RL_2^2 + F_1 - k_4RO^+ + k'_4O^-, \tag{11}$$

$$dG/dt = -2k_2R'G^2 + 2k'_2R + k_5EL_2, \tag{12}$$

$$dO^+/dt = -k_4RO^+ + k'_4O^-, \tag{13}$$

$$dE/dt = \eta\gamma O^+ - k_7E, \tag{14}$$

$$dM/dt = \eta\gamma O^+ - k_8M, \tag{15}$$

$$dL_2/dt = -2k_3RL_2^2 + 2F_1 - k_5EL_2 + k_6L_1M - k'_6L_2M. \tag{16}$$

These equations can be somewhat simplified by invoking a quasi-steady-state approximation whereby all genetic and macromolecular variables are assumed to adjust instantaneously to the metabolite concentrations. The validity of this approximation rests on the usually small average concentrations of macromolecules as opposed to the metabolite concentrations, as well as on the occurrence of fast steps in the decomposition on the intermediate enzymatic complexes.

Setting

$$\mu = k'_1 + k'_2, \tau = k_1R' + F_1 \text{ and } k_7 = k_8, \tag{17}$$

we obtain the reduced set:

$$\frac{dG}{dt} = -2k_2R'G^2 + \frac{2k'_2(k_2R'G^2 + \tau)}{(k_3L_2^2 + \mu)} + \frac{k_5L_2\eta\gamma k'_4\chi(k_3L_2^2 + \mu)}{k_7[k_4(k_2R'G^2 + \tau) + k'_4(k_3L_2^2 + \mu)]}, \tag{18}$$

$$\frac{dL_2}{dt} = -2k_3L_2^2\frac{(k_2R'G^2 + \tau)}{(k_3L_2^2 + \mu)} + 2F_1 + \frac{[k_6L_1 - (k_5 + k'_6)L_2]\eta\gamma k'_4\chi(k_3L_2^2 + \mu)}{k_7[k_4(k_2R'G^2 + \tau) + k'_4(k_3L_2^2 + \mu)]}. \tag{19}$$

These equations have been solved numerically on a CDC computer using Bairtow's method. The behaviour around the steady states has been studied via Merson's method. Note that the values of G, L_2, etc. at the steady states are completely independent of the quasi-steady-state approximation. On the other hand, the latter is instrumental in enabling one to investigate the *stability properties* of the steady states.

Whenever it was possible the values of the various constants have been chosen in agreement with the experimental results, as discussed in the appendix.

3. Multiple limit cycles and threshold phenomena

For a wide range of values of the different constants and for $k'_1 > 0.1$ one finds for the system of equations (18) and (19) a single stable steady state which behaves like a focus. Keeping all other constants fixed but taking $0.000248 \leqslant k'_1 \leqslant 0.1$ one finds a *stable focus* surrounded by *two* limit cycles (fig. 2): an unstable one, with a period around 110 min and a stable one with a period of 300 min. The time evolution of the concentrations is shown on figs. 3 and 4. We see that in the immediate vicinity of and inside the unstable cycle the system spires during several periods before being attracted to the stable steady state. Thus, the unstable cycle is quite relevant as far as the time dependent properties of the system are concerned. On the other hand, initial conditions close to but outside the unstable cycle are attracted to the outer (stable) limit cycle.

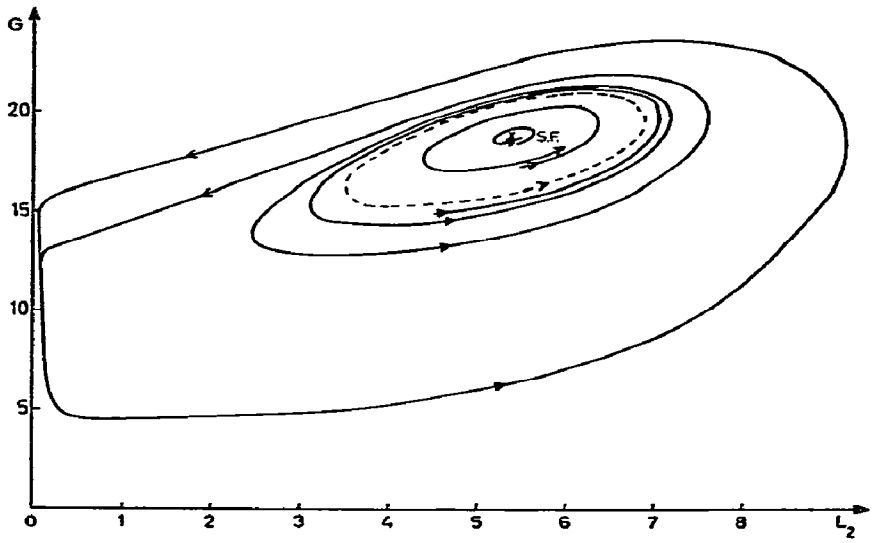

Fig. 2. Periodic trajectory in the phase space spanned by L_2 and G. Numerical values: $k_1 = 0.2\ \text{min}^{-1}$, $k'_1 = 0.008\ \text{min}^{-1}$, $R' = 10^{-2}\ \mu\text{M}$, $k_2 = 0.03\ \text{min}^{-1}\ \mu\text{M}^{-2}$, $k'_2 = 10^{-8}\ \text{min}^{-1}\ \mu\text{M}$, $k_3 = 0.2\ \text{min}^{-1}\ \mu\text{M}^{-2}$, $k'_3 = 6.0\ \text{min}^{-1}$, $F_1 = 10^{-3}\ \mu\text{M}$, $k_4 = 4 \times 10^{+5}\ \text{min}^{-1}\ \mu\text{M}^{-1}$, $k'_4 = 0.03\ \text{min}^{-1}$, $\eta\gamma = 510^{-3}\ \text{min}^{-1}$, $k_5 = 5000\ \text{min}^{-1}$, $k_6 = 0.6\ \text{min}^{-1}\ \mu\text{M}^{-1}$, $k'_6 = 0.006\ \text{min}^{-1}\ \mu\text{M}^{-1}$, $k_7 = k_8 = 3 \times 10^{-6}\ \text{min}^{-1}$, $\chi = 2.002 \times 10^{-3}\ \mu\text{M}$. The unstable limit cycle is indicated by dotted lines.

Finally, for $k'_1 < 0.000248$ one finds multiple steady states, and in particular:

– a stable focus surrounded by an unstable limit cycle of a period of about 110 min,

– a saddle point,

– a stable node.

The most natural way to accomodate topologically these types of behaviour [12] is shown on figs. 5 and 6. In addition to an unstable limit cycle, the system now features a saddle-node separatrix loop. Owing to this

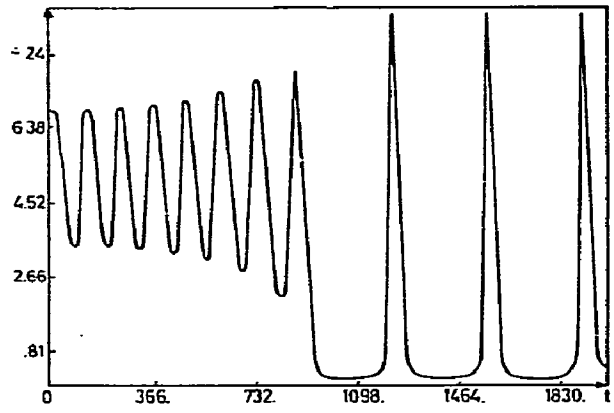

Fig. 3. Time evolution of the concentration L_2 with the same kinetic constants as in fig. 2. Initial values: $L_2^0 = 5.5\ \mu\text{M}$, $G^0 = 16\ \mu\text{M}$.

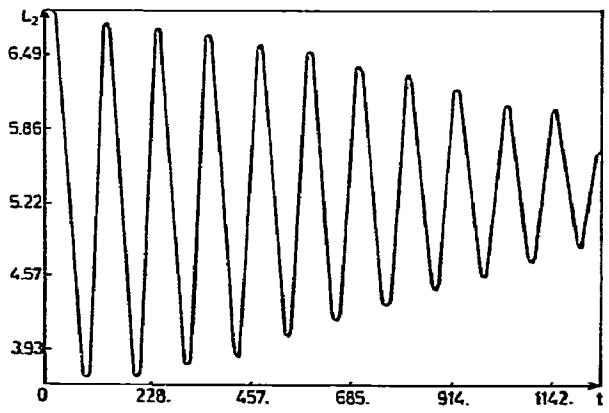

Fig. 4. Time evolution of the concentration L_2 with the same kinetic constants as in fig. 2. Initial values: $L_2^0 = 5.5\ \mu\text{M}$, $G^0 = 16.2\ \mu\text{M}$.

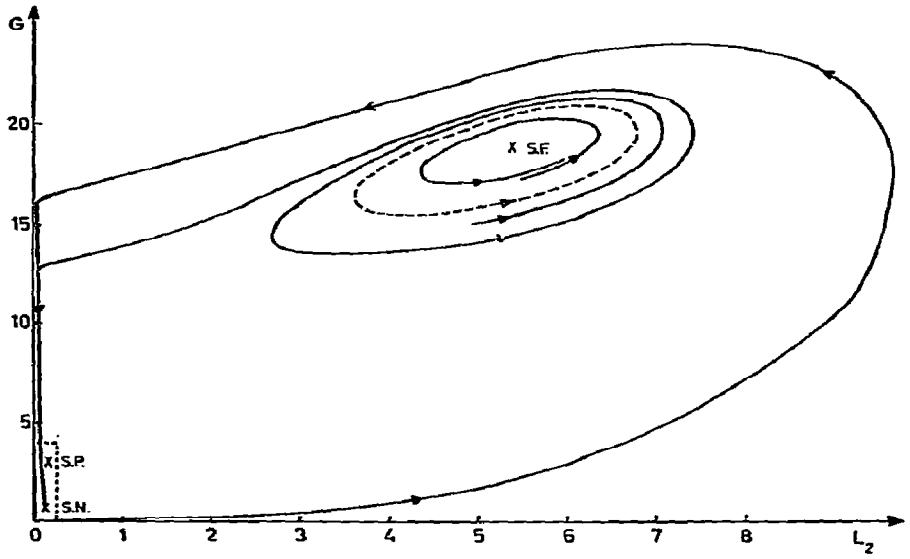

Fig. 5. Phase space representation of the evolution of the concentrations L_2 and G with same kinetic constants as in fig. 2 except $k'_1 = 10^{-5}$ min^{-1}. The unstable limit cycle is indicated by dotted lines.

closed (but unstable) trajectory, for certain initial conditions the system evolves for quite a long time before being atrracted by the stable node as indicated clearly on fig. 5 and 6.

The value $k'_1 \approx 0.000248$ min^{-1} has been determined approximately as the threshold value where the saddle point and the node merge to give rise to a multiple singular point of the saddle-node type. This threshold separates the multiple limit cycle from the multiple steady state regime.

For other sets of values of the parameters the system features a single asymptotically stable limit cycle of a period of about 160 min surrounding an unstable focus. The various possibilities found upon exploring the parameters $k_1, k'_1, k_2, k_5, L_1, F_1$ are compiled on table 1.

4. Discussion

Unstable limit cycles corresponding to subcritical branches bifurcating from steady states have already been found in chemical reactor theory [13]. Their existence is due to the *exponential* nonlinearity arising from the temperature dependence of the rate constants. We believe that our results are the first to establish the existence of unstable limit cycles as well as of multiple ones in isothermal systems undergoing mass-action kinetics, i.e., in systems subject to *polynomial* nonlinearities *.

From a general standpoint, we feel that multiple limit cycle behavior has some interesting implications. For instance, a system at a *stable* steady state surrounded by two limit cycles is endowed by an intrinsic *excitability*, in the sense that perturbations from this state exceeding a certain threshold evolve to a stable periodic regime instead of decaying back to the reference state. Excitability and threshold phenomena are widely spread in biology [6]. It seems therefore reasonable to expect that multiple limit cycles which, together with multiple steady states are the two alternatives for explaining this type of behavior, will play an increasingly important role in biochemical kinetics. Next, multiple limit cycles provide an efficient regulatory mechanism for varying the period of an oscillatory motion over a wide range values. Of equal im-

* This work was completed when we became aware of a Ph.D. Dissertation by J.A. Stanshine (M.I.T., Math. Department) who points out the existence of one unstable and one stable limit cycle in the Field–Noyes model for the Belousov–Zhabotinski reaction.

Table 1

k_1 (min^{-1})	F_1 (μM)	k_2 ($min^{-1}\mu M^{-2}$)	L_1 (μM)	k_5 ($min^{-1}\mu M^{-1}$)	k'_1 (min^{-1})	Steady states
0.2	6×10^{-3}	0.03	91100	5000	0.1	stable focus, no limit cycle
					0.097 0.008 0.000248	stable focus + unstable limit cycle ($T \approx 110$ min) + stable limit cycle ($T \approx 300$ min)
					0.000247 10^{-5}	stable focus + unstable limit cycle; saddle point; stable node
0.2	6×10^{-3}	0.003	51100	500	2.0	stable focus, no limit cycle
					0.1 0.008 0.000247	unstable focus + stable limit cycle ($T \approx 1500$ min)
					0.000248 10^{-5}	unstable focus; saddle point; stable node
0.02	6×10^{-4}	0.0003	99100	500	70	unstable focus + stable limit cycle ($T \approx 160$ min)
0.002	6×10^{-5}	0.003	99100	5000	2	stable focus, no limit cycle

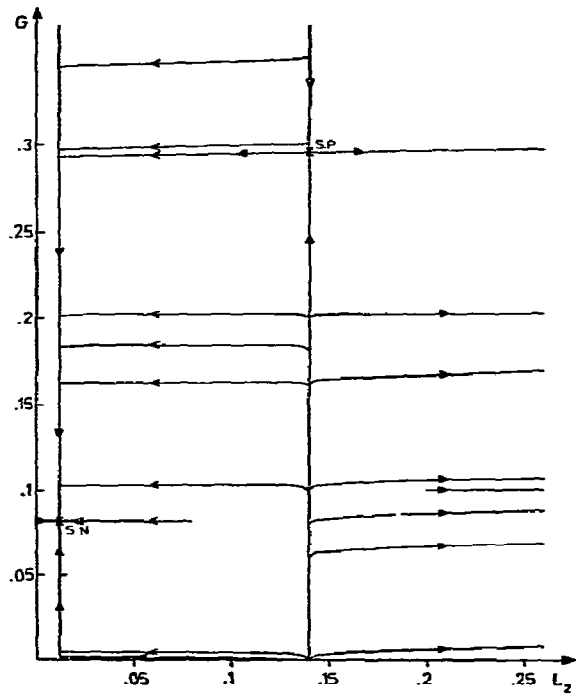

Fig. 6. Magnified phase space diagram around the node and the saddle point with the same kinetic constants as in fig. 5.

portance may be the overshoot behavior exhibited by the concentrations during the evolution depicted in fig. 5. Finally, just like in the case of bifurcation of spatial dissipative structures [14], the multiplicity of periodic trajectories provides a fascinating mechanism for a gradual complexification of a system evolving via a succession of instabilities under non-equilibrium conditions.

Let us come now to the more specific problem of the lac operon regulation. The periodic synthesis of β-galactosidase in *E. coli* has been observed both by Goodwin [15] in synchronous cultures and by Knorre [7] in asynchronous cultures. Masters and Donachie [16] found that the periodic synthesis of various enzymes in synchronous populations of *Bacillus Subtilis* arises from a variation in the repressor concentrations. Thus, it appears that the oscillatory enzyme synthesis is not a direct consequence of DNA replication. Rather, it reflects the intrinsic regulatory mechanisms involved in the synthesis. However, the period of the oscillation is of the same order of magnitude as the generation time. This is in qualitative agreement with our model which predicts a period of 110 min on the unstable limit cycle and of 160 min on the (unique) stable limit cycle corresponding to one of the sets of parameter values in table 1. Another point of agreement [15] is the increase of the frequency of oscillations as the external lactose concentration increases.

In spite of the endogenous character of the oscilla-

tions predicted by the model, it is quite possible that these oscillations can be influenced by the cell cycle. This should be especially so in synchronous cultures, whereas in asynchronous ones damped oscillations arising from destructive interference of the individual control circuits should be expected. Again, this is in qualitative agreement with Goodwin's observations [15] who pointed out that oscillations in synchronous cultures tend to be very stable. A detailed model coupling the lac operon regulatory circuit with the cell cycle is in progress [11].

From the experimental data is does not seem possible to draw definite conclusions as regards the threshold and excitability phenomena referred to in the beginning of this section. Nevertheless, some relevance could be possibly attached to the prediction of our model that the existence as well as the characteristics of the oscillations seem to be rather sensitive functions of such factors as the repression or induction conditions. In particular, a small change in the balance between repression and induction in a certain critical region should be sufficient to remove the system from the oscillatory regime and lead it to a steady state.

Acknowledgement

It is gratefully acknowledged that the early stages of this investigation have been carried out in collaboration with Dr. A. Babloyantz. We are also indebted to Professor R. Thomas and Drs. K. Kitahara and Th. Erneux for fruitful discussions.

Appendix: Numerical values of the various constants

A.1. Concentrations

According to ref. [17, 18], the concentration of the total amount of repressor is about 10^{-2} μM/ℓ and the concentration of the free repressor is almost the same as the total value. Thus, we choose

$$R' \approx 10^{-2}\ \mu\text{M}/\ell. \qquad \text{(A.1)}$$

Moreover, it is known [19] that in the non-induced state the concentration of the free operator (O^+) is 2×10^{-6} μM/ℓ whereas that of the operator–repressor complex (O^-) is 2×10^{-3} μM/ℓ. Thus, the total amount of operator is chosen to be:

$$\chi = O^+ + O^- = 2.002 \times 10^{-3}\ \mu\text{M}/\ell. \qquad \text{(A.2)}$$

The concentration of the repressor–inducer complex F is determined to be [17]

$$[RI] = F_1 \approx 10^{-3}\ \mu\text{M}/\ell. \qquad \text{(A.3)}$$

For reference, we also give here the values of E and inducer found in the computer simulations in a simplified model with a gratuitous inducer and without glucose [11]:

$[E] = 2\ \mu\text{M}/\ell$ (induced state)

$= 8.3 \times 10^{-3}\ \mu\text{M}/\ell$ (non-induced state).

$[L_2] = 3 \times 10^4\ \mu\text{M}/\ell$ (induced state)

$= 3.6\ \mu\text{M}/\ell$ (non-induced state)

The values of $[E]$ are in good qualitative agreement with the experimental value of 3.3 μM/ℓ for the induced state [21].

Note that the numerical values for E found in the present paper (i.e., with the effect of catabolite repression) are *smaller* than the preceding values. This seems natural, in view of the enhancement of the repressor concentration arising from the catabolite repression.

Coming now to the enzyme synthesis, experimental results show that the rate of β-galactosidase synthesis is proportional to the concentration of the free operator, and that the latter decreases with the repressor concentration. This is in qualitative agreement with eqs. (11) to (16). Indeed, when the quasi-steady state assumption is made on these equations one finds:

$$E = \eta\gamma O^+/k_7\,,$$

$$\text{and} \quad O^+ = k_4'\chi/k_4 R + k_4'\,. \qquad \text{(A.5)}$$

Implicitly, this result provides also a justification of condensing the complex process of enzyme synthesis in a single step. In this latter step we take, for the average concentration of the amino-acid pool:

$$\eta = 10^3\ \mu\text{M}/\ell. \qquad \text{(A.6)}$$

A.2. Rate constants

According to Bourgeois and coworkers [19], the association and dissociation constants of the repressor–operator reaction are *in vitro*:

$$k_4 = 4 \times 10^5 \text{ min}^{-1}\ \mu\text{M}^{-1}\,, \qquad k_4' = 0.03 \text{ min}^{-1}. \tag{A.7}$$

They also analyzed the repressor–inducer kinetics [10] and confirmed that the lac repressor interacts with two IPTG molecules [18, 20]. The corresponding rate constants are:

$$\text{association contact:} \quad k_3 = 0.2 \text{ min}^{-1}\ \mu\text{M}^{-2}\,,$$

$$\text{dissociation constant:} \quad k_3' = 6.0 \text{ min}^{-1}\,. \tag{A.8}$$

The rate constant for the glucose–inactive repressor reaction is not known experimentally. In fact this reaction is the overall result of several intermediate steps involved in catabolite repression, in which c-AMP plays an important role *. Still, it appears plausible to postulate that the association constant is of the same order of magnitude as in the repressor–inducer reaction. Thus we take

$$k_2 \approx 0.03 \text{ min}^{-1}\ \mu\text{M}^{-2} \tag{A.9}$$

for most of our simulations, and subsequently vary k_2 by two orders of magnitude along with other parameters appearing in table 1.

The overall rate of enzyme synthesis is hard to determine on the basis of the global step (5). It appears reasonable to take a rate $\eta\gamma$ much larger than the dilution rate k_7 of the enzymes. Thus we choose:

$$\eta\gamma/k_7 = 10^3\,. \tag{A.10}$$

The precise value of the kinetic constant for the lactose degradation is not known. However, the reaction seems to be rather rapid. Thus we take

$$k_5 = 5 \times 10^2 \text{ to } 5 \times 10^3 \text{ min}^{-1}\ \mu\text{M}^{-1}\,. \tag{A.11}$$

Finally, the rate constants of the permease mediated transport have been calculated using Kepes' model [18, 22]. The following values have thus been determined:

$$k_6 = 0.6 \text{ min}^{-1}\ \mu\text{M}^{-1}\,, \qquad k_6' = 0.006 \text{ min}^{-1}\ \mu\text{M}^{-1}\,. \tag{A.12}$$

The asymmetry between the two constants is essential to ensure an abrupt transition from a non-induced state to an induced one in the presence of a gratuitous inducer like IPTG. We have extended our model to account for the details of the transport process using a mechanism suggested by Kepes [11]. We have verified that the qualitative behaviour remains the same as that reported in the present paper.

The remaining constants k_1, k_1', L_1, k_2, k_5 have been used as parameters in the computer simulations and varied over a wide range of values as reported in the figure captions and in table 1.

It should be pointed out that the values of the kinetic constants depend also on environmental factors like temperature, pH, etc., which are not considered explicitly in this paper. However, we have performed an implicit test of our choice of numerical values as follows [11]. We have studied the *kinetics* of the pure induction process in the presence of a gratuitous sugar (i.e., without the glucose effect). We have verified that the time evolution of the induced enzyme concentration is in good agreement with the experimentally known behavior.

References

[1] P. Glansdorff and I. Prigogine, Thermodynamic Theory of Structure, Stability and Fluctuations (Wiley, New York, 1971).
[2] G. Nicolis and I. Prigogine, in: Proceedings 9th Faraday Symposium, London (1974).
[3] A. Goldbeter and R. Lefever, Biophys. J. 12 (1972) 1302.
[4] C. Walter, J. Theor. Biol. 23 (1969) 23; 27 (1970) 259.
[5] A. Goldbeter, Ph.D. Dissertation, University of Brussels (1973).
[6] B. Hess and A. Boiteux, Ann. Rev. Biochem. 40 (1971) 237.
[7] W.A. Knorre, Bioch. Bioph. Res. Comm. 31 (1968) 812.
[8] A. Babloyantz and M. Sanglier, FEBS Letters 23 (1972) 364.
[9] J. Palmer and V. Mose, Biochem. J. 106 (1968) 339.
[10] S. Bourgeois and J. Monod, Ciba Symposium on Control Processes in Multicellular Organisms.
[11] M. Sanglier, Ph.D. Dissertation, University of Brussels (1976).
[12] A.A. Andronov, A.A. Vitt and S.E. Khaikin, Theory of Oscillators (Pergamon Press, Oxford, 1966).
[13] See, e.g., D.S. Cohen, in: Springer Tracts in Applied Mathematics, Vol. 309 (Springer, Berlin, 1973).
[14] G. Nicolis and J.F.G. Auchmuty, PNAS 71 (1974) 2748.
[15] B.C. Goodwin, European J. Biochem. 10 (1969) 515.
[16] M. Masters and W.D. Donachie, Nature 209 (1966) 476.
[17] B. Muller-Hill, Angew. Chem. Intern. Edit. Vol. 10 (1971) 160.

[18] J. Beckwith and D. Zipser, eds. Lactose Operon (Cold Spring Harbor Laboratory, New York, 1970).
[19] A.D. Riggs, S. Bourgeois and M. Cohn, J. Mol. Biol. 53 (1970) 401.
[20] G. Yagil and E. Yagil, Biophys. J. 11 (1971) 11.
[21] J. Watson, Molecular Biology of the Gene (Benjamin, 1970).
[22] A. Kepes, Biochem. Biophys. Acta 40 (1960) 70.